Environ Sci Pollut Res
DOI 10.1007/s11356-017-8412-z

RESEARCH ARTICLE

Effectiveness of SO_2 emission control policy on power plants in the Yangtze River Delta, China—post-assessment of the 11th Five-Year Plan

Jiani Tan[1] · Joshua S. Fu[1] · Kan Huang[1,2] · Cheng-En Yang[1] · Guoshun Zhuang[2] · Jian Sun[1]

Received: 31 July 2016 / Accepted: 5 January 2017

Abstract Facing the air pollution problems in China, emission control strategies have been implemented within the framework of national Five-Year Plan (FYP). According to the lack of post-assessment studies in the literature, this study assessed the effectiveness of the SO_2 emission control policies on power plants after the 11th FYP (2006–2010) by modeling emission control scenarios. The idealized emission control policy (the PS90 scenario with assumption of 90% SO_2 emission reduction from power plants) could reduce the SO_2 and SO_4^{2-} concentrations by about 51 and 14%, respectively, over the Yangtze River Delta region. While the actual emission control condition (the P2010 scenario based on the actual emissions from power plants in 2010) demonstrated that the actual reduction benefits were 30% of SO_2 and 9% of SO_4^{2-}. On the city scale, the P2010 scenario imposed positive benefits on Shanghai, Nanjing, Nantong, and Hangzhou with SO_2 reductions of about 55, 12, 30, and 21%, respectively, while an 11% increase of SO_2 concentration was found in Ningbo. The number of days exceeding China's National Ambient Air Quality Standard of Class I daily SO_2 concentration was estimated to be 75, 52, 7, 77, and 40 days for Shanghai, Nanjing, Nantong, Ningbo, and Hangzhou under the real SO_2 control condition (P2010). The numbers could be decreased by 16, 11, 2, 21, and 11% if the control effect reaches the level of the PS90 scenario. This study serves as a scientific basis to design capable enforcement of emission control strategies in China in the future national plans.

Keywords Post-assessment · Air quality modeling · 11th Five-Year Plan · SO_2 emission control · WRF/CMAQ · Yangtze River Delta

Responsible editor: Gerhard Lammel

Electronic supplementary material The online version of this article (doi:10.1007/s11356-017-8412-z) contains supplementary material, which is available to authorized users.

✉ Joshua S. Fu
jsfu@utk.edu

[1] Department of Civil and Environmental Engineering, The University of Tennessee, Knoxville, TN 37996, USA

[2] Department of Environmental Science and Engineering, Fudan University, Shanghai 200433, People's Republic of China

Introduction

China has been facing severe challenges of air pollution. In order to improve the air quality, the Chinese government has developed a series of emission control strategies in the national Five-Year Plans (FYP). During the 11th FYP (2006–2010), control policies on SO_2 emissions have been specifically implemented. An overall target was set to cut off 10% of the national SO_2 emissions from the 2005 level by the end of year 2010. By adopting new policies and installing control devices, this emission reduction goal has been successfully achieved with 14% reduction of the total SO_2 emissions (Schreifels et al. 2012). As a result, the SO_2 air pollution problem has been improved (Wang and Hao 2012). However, this improvement was achieved by multiple factors including the control policies of the 11th FYP, changes in the meteorology fields, and special events like the 2010 Shanghai Expo. The actual contributions of the control policies of the 11th FYP on improving the air quality still remain unclear.

Air quality models have been widely applied to assess the effects of emission control policies (Wang et al. 2010a, b, c, 2014, 2009; Xing et al. 2011b; Xue et al. 2013). Wang et al. (2010a, b) estimated the SO_2 emission in 2010 if the 11th FYP was not implemented. The predicted SO_2 emission under this

Published online: 03 February 2017

scenario is 52% higher than the estimated 2010 emission with the 11th FYP control. Also, the corresponding concentration reduction could reach 30–60% in the highly polluted area in Eastern China. Wang et al. (2013a) found that the SO_2 control policies during the 11th FYP have largely decreased the number of extremely heavy pollution days. Dong et al. (2013) demonstrated that emission reduction of SO_2 and NO_x could reduce the exceeding days of the new National Ambient Air Quality Standard (NAAQS) enacted in 2012. Joint control of SO_2 and NO_x emissions has significant improvements on the air quality. Wang et al. (2013b) investigated the sulfate–nitrate–ammonium aerosol response to SO_2 control strategy during the 11th FYP. The NO_3^- concentration would increase without additional control on NH_3 emissions, which would offset the benefits of SO_2 control on reducing $PM_{2.5}$ pollution. However, only few studies have conducted post-assessment on the effectiveness after the end of the target year.

In order to assess the control effectiveness, the method of modeling emission control scenarios was applied, which has been widely used to understand the corresponding changes of air pollution to changes of emissions (Streets and Waldhoff 2000; Xing et al. 2011a). In the design of emission control scenarios, due to lacking of actual working conditions of the emission control technologies, a uniform removal rate is usually applied to the emission inventory over the study domain to calculate the emissions after control. This method is widely used to predict the future emissions under various emission control scenarios to support the determination of future emission control policies. However, the post-assessment on a specific emission control policy requires high accuracy in the removal rate of emission. The traditional way of uniform removal rate generally has very high uncertainties. For instance, the Chinese authority announced a general reduction rate of 78.7% for the Flue Gas Desulfurization (FGD) in 2008, but there were doubts in both the operation time of the FGD and its removal rate (Xu 2011). Applying the uniform reduction rate also ignores the spatially differences of emission control effectiveness in different areas, which is caused by operation conditions such as the composition of exhaust gases.

This study conducted a post-assessment on the effectiveness of the SO_2 control policies on power plants at the end of the 11th FYP over the Yangtze River Delta (YRD) region. Three scenarios were simulated, including the SO_2 emission condition in 2006 (Base Case scenario), optimal SO_2 reduction condition in 2010 assuming the SO_2 removal efficiency of FGDs on power plant outlets could reach 90% (PS90 scenario), and estimation of the SO_2 emission status from power plants in 2010 (P2010 scenario). All of the three scenarios were simulated with the meteorology of 2006, when these scenarios were designed and conducted. The benefits and effectiveness of the SO_2 control policies were evaluated and reviewed in 2010, which is the end of the 11th FYP. The results also quantified the contributions of these control policies on improving the SO_2 pollution problem after 5 years of implementation.

Methodology

Model description

The Weather Research and Forecasting (WRF) model version 3.5.1 was used to simulate the meteorological field. Initial and boundary conditions were provided by Final Analyses (FNL) 1 × 1° data from the National Centers for Environmental Prediction (NCEP). Simulations were run on one-way nested grids with resolutions of 27, 9, and 3 km for the whole year of 2006. Table 1 lists the model configuration for the 3-km-resolution grid. Output files were processed by the Meteorology-Chemistry Interface Processor (MCIP) version 4.2 to provide meteorological inputs for air quality model.

The Community Multi-scale Air Quality Model (CMAQ) version 5.0.2 was applied to predict the regional air quality. The model contains several processors, including meteorology-chemistry interface processor (MCIP), photolysis rate processor (JPROC), initial conditions processor (ICON), boundary conditions processor (BCON), and CMAQ chemical-transport model (CCTM). The gas-phase chemical mechanism, aerosol mechanism, and liquid-phase chemical mechanism used in the model configuration were Carbon Bond Mechanism (CB05), AERO6, and Cloud_acm_ae6. The vertical profile contained 19 layers, with denser layers at lower altitudes.

Figure 1a shows the simulation domains. The 27-km domain covered the whole China and the surrounding areas, the 9-km domain included Eastern China, and the 3-km domain was the focus of this study, e.g., the YRD region. The administrative boundaries of cities within the YRD region are illustrated in Fig. 1b. Chemical initial and boundary conditions for the 27-km domain were downscaled from the GEOS-Chem global model results (Lam and Fu 2009). The boundary conditions for the 9- and 3-km nested domains were generated from the mother domains by the BCON processor.

Emission inventory and emission control scenario

The emission inventory was based on the INTEX-B anthropogenic emission inventory of 2006 (Zhang et al. 2009). It has been widely used to study the air pollution problems in Asia (Dong et al. 2013, 2014; Han et al. 2011, 2015). Although this inventory was developed for air pollutant emissions in 2006, the statistical data used was mostly from 2004 or 2005 for most of the Asian countries (Zhang et al. 2009). Thus, the amounts of SO_2 emissions from power plants in this inventory were collected or calculated before the installation of FGDs started in 2006. Du (2008) integrated this inventory with

Table 1 Main physics options of WRF model for 3-km-resolution grid

Physics options	Options used for 3-km-resolution grid
Microphysics (mp_physics)	(8) New Thompson et al. scheme
Longwave Radiation (ra_lw_physics)	(4) RRTMG scheme
Shortwave Radiation (ra_sw_physics)	(4) RRTMG shortwave
Surface Layer (sf_sfclay_physics)	(1) MM5 similarity
Land Surface (sf_surface_physics)	(1) Noah Land Surface Model
Planetary Boundary layer (bl_pbl_physics)	(1) Yonsei University scheme
Cumulus Parameterization (cu_physics)	Not used
Analysis Nudging Runs (grid_fdda)	0

biogenic from Global Emission InitiAtive (GEIA), biomass burning, and ship emissions from Transport and Chemical Evolution over the Pacific (TRACE-P). The updated emission inventory was used for model simulation in this study.

According to the governmental report (SCPRC 2006) and related studies (Cao et al. 2009; Wang and Hao 2012; Zhao et al. 2008), two major policies have been implemented to control the SO_2 emissions during the 11th FYP. One policy was to install the FGD technology on the coal-fired power plants to remove SO_2 emissions from exhaust gases. The other policy was to shut down the small power plants with low combustion efficiencies. Both policies focused on the power plant sector, which accounted for 65% of the total SO_2 emissions in the YRD region in 2006. In this study, we also focused on the emission control policies implemented on the power plant sector.

Three emission control scenarios were simulated as described in Table 2. The first scenario, referred to the Base Case scenario, used the 2006 emission inventory. The simulation result of this scenario represented the prediction of SO_2 concentration in 2006. The second scenario was referred to the PS90 scenario. This scenario assumed an idealized emission control condition that FGDs were installed on all of the existing power plants and worked with a theoretical SO_2 emission removal efficiency of 90% (Srivastava and Jozewicz 2001; Srivastava et al. 2001). The policy of shutting down some small power plants was not considered in this scenario due to lacking related information. The SO_2 emissions from the other sectors besides the power plant sector were the same as the 2006 emission inventory. The SO_2 concentration simulated under this scenario was supposed to be lower than that under the Base Case scenario. The negative difference between the two (PS90 − Base Case) denoted the optimal control effectiveness of the idealized emission control policies on reducing the SO_2 concentration. The third scenario was referred to the P2010 scenario. It used the emission from power plants in 2010 from Fu et al. (2013) and emissions from

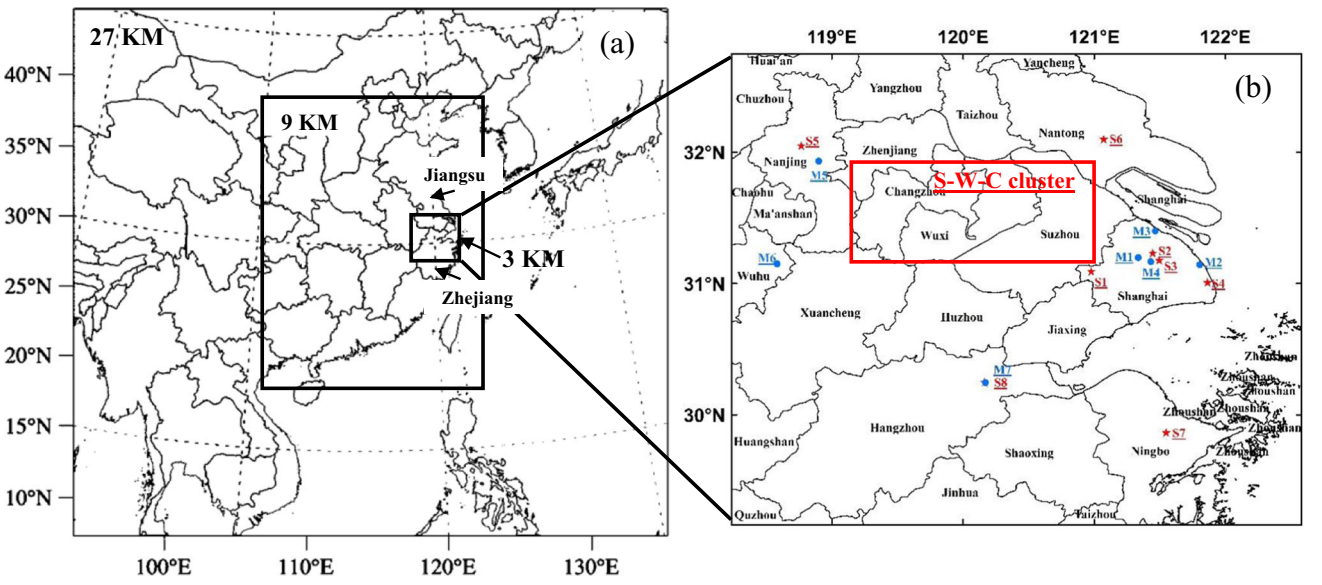

Fig. 1 **a** Simulation domains. **b** Research domain and administrative boundaries of main cities. Meteorology stations are represented by *blue circle*. Markers: *M1* Hongqiao Airport, *M2* Pudong Airport, *M3* Fudan University Station, *M4* Xuhui Station, *M5* Nanjing Station, *M6* Wuhu Station, *M7* Hangzhou Station. Air pollution monitoring stations are represented by *red star symbols*: *S1* Shanghai, *S2* Nanjing, *S3* Nantong, *S4* Ningbo, *S5* Hangzhou (the same position as M7)

Table 2 Description of emission control scenarios in this study

Scenario name	Emission input		Meteorology input	Description
	Power plant	Other emission sectors		
Base Case	2006 baseline	2006 baseline	2006 baseline	Control case
PS90	2006 baseline × optimal reduction rate	2006 baseline		Optimal power plant emission control scenario in 2010
P2010	2010 emission data	2006 baseline		Actual power plant emission control condition in 2010

other sectors remained the same as the Base Case scenario. This emission scenario reflected the actual SO_2 emission control status on power plants in 2010. Simulation result of this scenario was not the prediction of SO_2 concentration in 2010, but the difference in SO_2 concentration between this scenario and Base Case scenario reflects the real SO_2 reduction effectiveness of the emission control policies at the end of the 11th FYP. Figure S1 shows the annual SO_2 emission over the YRD region under the three scenarios. The annual SO_2 emission under the Base Case scenario was 2046 kt, of which 1320 kt was from the power plant sector. The emission from power plants was reduced to 132 kt under the PS90 scenario and the total SO_2 emission was 858 kt. Under the P2010 scenario, the total SO_2 emission was 1737 kt, with 1011 kt contributed by the power plant sector.

Observation data

On-site observation data was used to evaluate the WRF and CMAQ model performances in 2006. The locations of the observation stations are indicated in Fig. 1b. Meteorological data was available in seven stations from the National Climate Data Center (NCDC). The seven stations included Hongqiao airport station in Shanghai (M1), Pudong airport station in Shanghai (M2), Fudan University station in Shanghai (M3), Xuhui station in Shanghai (M4), Nanjing station in Jiangsu Province (M5), Wuhu station in Anhui Province (M6), and Hangzhou station in Zhejiang Province (M7). The meteorological factors evaluated were daily averaged temperature at 2 m height (T2), wind speed and wind direction at 10 m height (WS10 and WD10), and water content.

Daily average SO_2 and NO_2 observation data in 2006 at Shanghai station (S1) was provided by Shanghai daily air quality report from the Shanghai Environmental Monitor Center (SEMC 2015). Daily average SO_2 observation data in 2010 was available from Lin et al. (2013) for five stations, including Shanghai (S1), Nanjing (S2), Nantong (S3), Ningbo (S4), and Hangzhou (S5). Daily averaged concentrations of inorganic $PM_{2.5}$ compositions, including NO_3^-, SO_4^{2-}, and NH_4^+, were available from site sampling at Fudan University station (M3) for the whole month of August in 2006. The monthly average SO_2 observation from remote sensors of Ozone Monitoring Instrument (OMI) was employed to compare with the modeled SO_2 vertical column density (VCD).

Results and discussion

Model result evaluation

Table 3 summarizes the model performance of meteorological field. WS10 was in good accordance with observation data. The annual mean bias (MB) and root mean square error (RMSE) were 0.19 and 0.66 m/s. The temporal variation was well captured with the *R* (correlation coefficient) value reaching 0.81. February, March, April, and November were overestimated in the WS10 by 0.88, 0.29, 0.47, and 0.39 m/s, while June and July were underestimated by 0.28 and 0.36 m/s. The *R* values in February, March, and April were only 0.61, 0.67, and 0.38, far below the average value of 0.81. The MB of WD10 is −4.15°, ranging from −0.57 to 11.49°. T2 was overestimated by 1.01 °C, especially in February (3.25 °C), March (3.05 °C), and April (2.23 °C). The temporal variation was well simulated with *R* value of 0.99. Water content was slightly underpredicted by 0.62 g/kg. Overall, the WRF model produced reasonable meteorology field for the CMAQ simulation.

Model performances in simulating the concentrations of SO_2, NO_2, and major $PM_{2.5}$ inorganic components (SO_4^{2-}, NO_3^-, and NH_4^+) in 2006 were evaluated with observation data in Fig. 2, Fig. 3, and Table 4. SO_2 was generally well simulated with annual mean bias of −1.58 μg/m^3. The temporal variation was well reproduced throughout the whole year, and the high concentration peaks were captured in most times (Fig. 2a). The SO_2 concentrations were underestimated in March (23.30 μg/m^3), April (9.15 μg/m^3), and November (8.77 μg/m^3), partly due to the overestimation of wind speed and model bias in simulating the wind direction. The annual RMSE value is 30.80 μg/m^3, ranging from 14.75 μg/m^3 in July to 32.09 μg/m^3 in December. The scatter plot of SO_2 (Fig. 3a) shows that most data points lie between the 1:2 and 2:1 ratio lines. The regression slope between model result and observation was 0.85, indicating good consistency between

Table 3 Model performance of temperature at 2 m height (T2), wind speed at 10 m height (WS10) and wind direction at 10 m height (WD10), and water content in 2006

		Observation average	Model average	MB[a]	NMB[a] (%)	NME[a] (%)	MFB[a] (%)	MFE[a] (%)	RMSE[a]	R^{2a}
WS10 (m/s)	Annual	3.26	3.44	0.19	5.76	13.99	4.46	13.43	0.66	0.66
	JAN	3.50	3.67	0.17	4.73	8.38	2.75	8.20	0.40	0.94
	FEB	2.94	3.82	0.88	29.91	38.19	21.13	30.97	1.37	0.37
	MAR	2.98	3.28	0.29	9.88	21.73	6.11	20.04	0.82	0.45
	APR	3.18	3.65	0.47	14.85	26.59	10.27	23.08	1.08	0.14
	MAY	3.65	3.92	0.27	7.32	10.69	7.71	11.23	0.59	0.77
	JUN	3.22	2.93	−0.28	−8.80	9.48	−9.83	10.47	0.37	0.88
	JUL	3.86	3.50	−0.36	−9.32	10.86	−9.66	11.58	0.52	0.94
	AUG	3.37	3.45	0.08	2.52	7.08	2.82	7.41	0.34	0.86
	SEP	3.34	3.37	0.03	1.02	7.37	1.49	7.26	0.31	0.86
	OCT	2.81	2.94	0.13	4.69	8.76	4.54	8.89	0.29	0.77
	NOV	3.23	3.62	0.39	12.05	13.37	9.89	11.71	0.56	0.92
	DEC	2.95	3.18	0.23	7.96	11.64	7.68	12.06	0.38	0.92
WD10 (°)	Annual	179.34	144.66	4.15	2.32	4.72	7.32	10.77	10.42	–
	JAN	160.59	132.10	9.16	5.71	7.64	19.13	21.75	13.85	–
	FEB	193.81	118.87	3.25	1.68	2.28	7.44	8.03	5.87	–
	MAR	247.82	148.79	3.06	1.23	2.64	3.42	5.13	7.73	–
	APR	241.71	184.97	5.34	2.21	2.93	2.88	3.81	9.41	–
	MAY	170.06	155.19	1.09	0.64	5.19	2.04	8.27	12.57	–
	JUN	156.39	145.85	−0.57	−0.36	5.62	2.17	9.53	12.43	–
	JUL	164.07	153.78	−0.20	−0.12	4.20	−0.97	4.48	9.34	–
	AUG	154.25	125.51	1.83	1.18	4.31	2.33	7.42	8.75	–
	SEP	109.75	91.13	3.10	2.82	5.82	3.89	11.47	8.16	–
	OCT	130.76	93.36	6.28	4.80	6.58	17.28	19.04	10.99	–
	NOV	192.99	179.78	5.98	3.10	4.18	14.92	16.86	10.64	–
	DEC	230.77	204.82	11.49	4.98	5.26	13.31	13.49	15.25	–
T2 (°C)	Annual	16.74	17.75	1.01	6.02	7.71	25.00	26.31	1.86	0.98
	JAN	5.34	5.88	0.54	10.14	12.88	80.50	82.13	0.83	0.98
	FEB	2.32	5.57	3.25	140.07	140.07	144.92	144.92	3.73	0.69
	MAR	8.03	11.08	3.05	37.98	39.11	35.98	37.04	3.48	0.76
	APR	14.10	16.33	2.23	15.79	16.61	13.96	14.76	2.94	0.69
	MAY	20.47	20.65	0.18	0.88	3.44	1.01	3.57	0.87	0.90
	JUN	25.35	25.70	0.34	1.35	2.88	1.34	2.90	0.86	0.94
	JUL	28.78	28.74	−0.04	−0.14	1.98	−0.14	1.99	0.67	0.85
	AUG	29.49	29.12	−0.36	−1.24	2.10	−1.24	2.10	0.71	0.72
	SEP	23.02	23.42	0.40	1.74	2.85	1.84	2.94	0.81	0.92
	OCT	21.19	21.54	0.34	1.62	2.78	1.79	2.89	0.73	0.92
	NOV	14.59	15.61	1.01	6.94	6.94	7.52	7.52	1.17	0.98
	DEC	7.18	8.54	1.36	18.98	19.19	21.70	21.89	1.51	0.94
Water content (g/kg)	Annual	10.64	10.02	−0.62	−5.86	8.94	−6.00	10.59	1.30	0.96
	JAN	4.59	4.46	−0.12	−2.67	4.73	−4.87	6.83	0.28	0.98
	FEB	4.10	4.03	−0.08	−1.88	15.87	−5.95	16.76	0.82	0.86
	MAR	4.84	4.90	0.06	1.29	17.64	−4.04	18.96	1.03	0.79
	APR	6.93	7.36	0.43	6.27	18.67	1.92	17.74	1.75	0.56
	MAY	11.18	10.20	−0.99	−8.84	9.56	−9.97	10.62	1.25	0.86
	JUN	16.35	13.92	−2.43	−14.86	14.86	−16.58	16.58	2.68	0.83
	JUL	20.40	18.98	−1.43	−6.98	7.11	−7.40	7.53	1.70	0.62
	AUG	19.98	19.21	−0.77	−3.86	4.47	−3.80	4.54	1.00	0.86
	SEP	13.97	13.24	−0.73	−5.25	5.76	−5.36	5.98	0.96	0.94
	OCT	12.22	11.36	−0.86	−7.02	7.12	−7.02	7.16	1.04	0.90
	NOV	7.76	7.24	−0.52	−6.66	8.07	−7.69	9.06	0.84	0.86
	DEC	4.80	4.77	−0.03	−0.67	5.71	−1.40	6.20	0.41	0.92

[a] The indexes are defined as below (*n* size of samples, *mod* model results, *obs* observation data):

MB (mean bias) $= \frac{1}{n}\sum_1^n (mod - obs)$;

NMB (normalized mean bias) $= \frac{\sum_1^n (mod - obs)}{\sum_1^n obs} \times 100$

NME (normalized mean error) $= \frac{\sum_1^n |mod - obs|}{\sum_1^n obs} \times 100$;

MFB (mean fractional bias) $= \frac{1}{n}\sum_1^n \frac{mod - obs}{(mod + obs)} /2 \times 100$

MFE (mean fractional gross error) $= \frac{1}{n}\sum_1^n \frac{|mod - obs|}{(mod + obs)} /2 \times 100$

RMSE (root mean square error) $= \sqrt{\frac{1}{n}\left(\sum_1^n (mod - obs)^2\right)}$

R^2 (coefficient of determination)

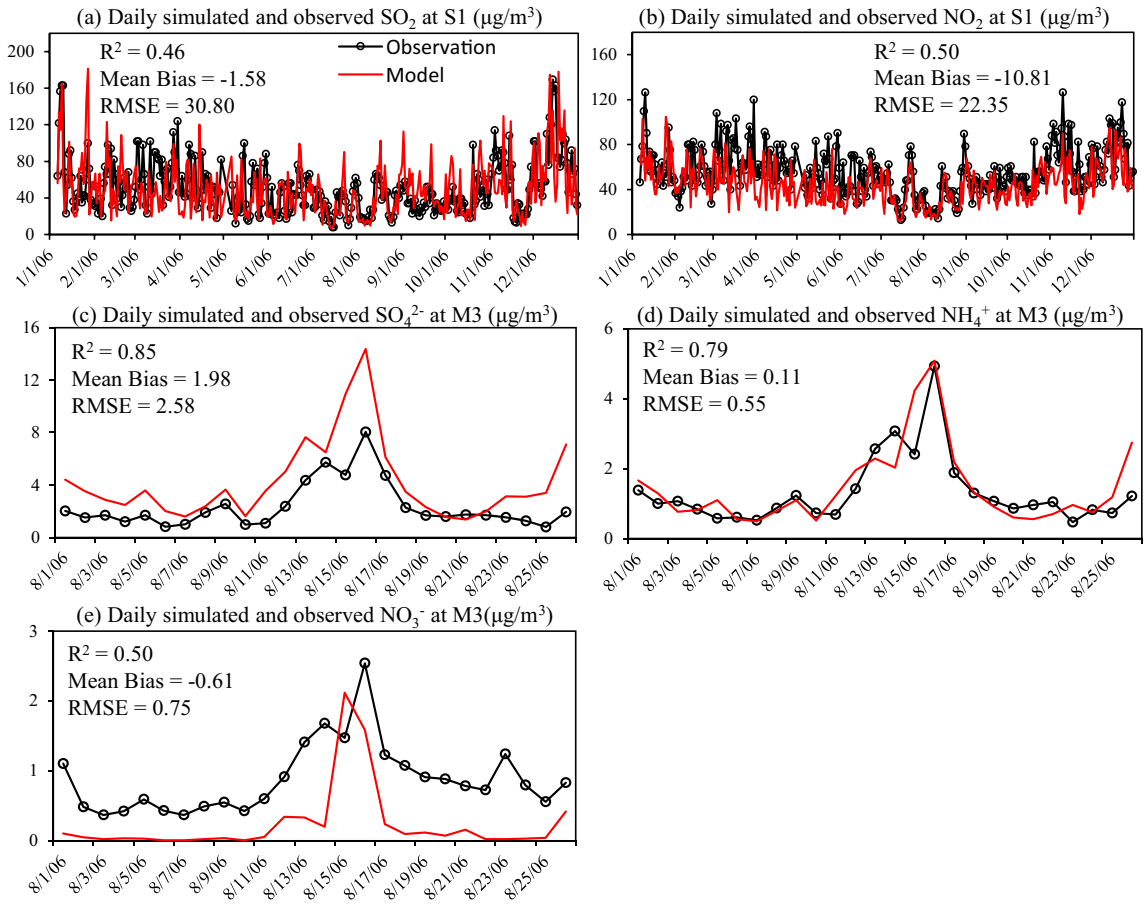

Fig. 2 Daily simulated and observed **a** SO_2 and **b** NO_2 at S1, and **c** SO_4^{2-}, **d** NH_4^+, and **e** NO_3^- at M3. The *R* and mean bias values were calculated using the same equation as in Table 2

the model and observation. The simulated SO_2 VCDs were compared with OMI data in Fig. S2 in the supplementary material. The distribution of SO_2 concentration was in good accordance with OMI observation in YRD region.

NO_2 was underestimated by 10.81 μg/m^3, especially in March (21.63 μg/m^3), April (18.44 μg/m^3), and November (19.31 μg/m^3). In the other months, the model reproduced most of the concentration peaks successfully. The annual RMSE value is 22.35 μg/m^3, ranging from 11.72 to 32.09 μg/m^3. The result was similar to SO_2 to some extent. Meteorology inputs of wind speed and wind direction were also considered as the main reason for the underestimation of NO_2 concentration in these months. Most scatter points of NO_2 (Fig. 3b) were distributed between the 1:2 and 2:1 ratio lines, but closer to the 2:1 ratio line. The regression slope was 0.76, indicating general underestimation by the model.

Figure 2c to e show the model performance of major $PM_{2.5}$ inorganic components (SO_4^{2-}, NO_3^-, and NH_4^+) in August of 2006. High consistencies were found between the temporal variations of modeled species and those of

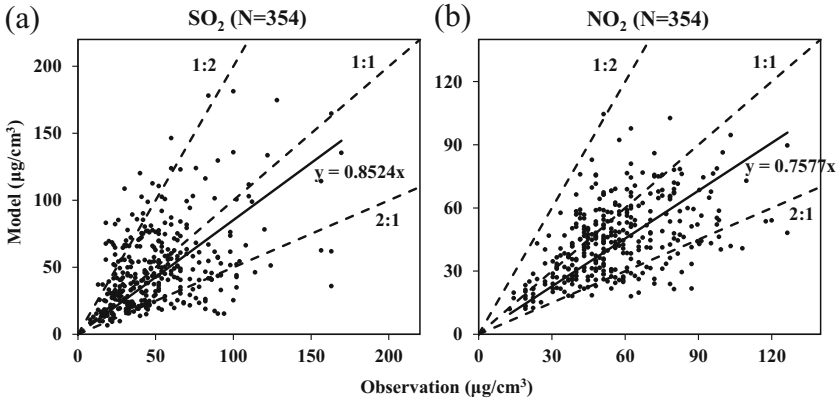

Fig. 3 Scatter plots of daily simulated versus observed **a** SO_2 **b** NO_2 at S1 station

Table 4 Model performance of SO_2 and NO_2 at Shanghai station in 2006

Pollutants		Average observation (μg/m^3)	Average model (μg/m^3)	MB (μg/m^3)	NMB (%)	NME (%)	MFB (%)	MFE (%)	RMSE (μg/m^3)
SO_2	Annual	50.9	49.3	−1.58	−3.11	44.74	−5.83	44.59	30.80
	JAN	67.7	71.0	3.26	4.82	41.69	1.61	42.65	39.36
	FEB	50.4	55.6	5.20	10.32	56.07	8.20	54.78	33.52
	MAR	70.0	46.7	−23.30	−33.27	39.70	−39.20	47.14	34.03
	APR	54.3	45.2	−9.15	−16.84	56.36	−24.71	62.26	36.97
	MAY	46.0	42.2	−3.75	−8.15	54.68	−5.74	53.41	33.13
	JUN	41.4	42.3	0.86	2.07	32.31	−3.21	33.69	18.26
	JUL	32.1	32.1	−0.01	−0.02	32.25	−6.06	32.62	14.75
	AUG	35.7	33.9	−1.71	−4.78	36.38	−13.18	35.82	18.10
	SEP	35.0	48.9	13.89	39.68	47.73	28.24	36.81	23.66
	OCT	38.8	49.1	10.29	26.55	51.43	14.52	43.24	25.08
	NOV	55.7	46.9	−8.77	−15.74	45.53	−17.32	50.62	31.08
	DEC	85.0	79.9	−5.08	−5.98	42.73	−11.37	45.02	46.80
NO_2	Annual	55.7	44.8	−10.81	−19.45	29.88	−21.27	33.03	22.35
	JAN	65.6	62.7	−2.89	−4.41	30.62	−4.25	29.40	27.56
	FEB	53.2	50.8	−2.43	−4.57	24.46	−3.27	25.45	16.58
	MAR	73.2	51.6	−21.63	−29.55	35.58	−34.84	42.09	32.09
	APR	62.1	43.7	−18.44	−29.69	37.52	−37.23	45.44	28.37
	MAY	55.2	37.2	−17.86	−32.44	43.67	−38.61	50.36	28.55
	JUN	49.7	38.3	−11.32	−22.79	29.91	−25.64	34.02	18.16
	JUL	39.4	32.0	−7.48	−18.97	23.59	−22.29	27.39	11.72
	AUG	35.4	28.8	−6.57	−18.58	27.36	−17.30	27.92	13.94
	SEP	45.4	40.2	−3.73	−8.49	24.12	−7.41	29.84	13.87
	OCT	50.5	43.3	−7.22	−14.29	24.84	−16.50	26.80	16.27
	NOV	68.4	49.1	−19.31	−28.23	31.39	−31.94	36.11	26.71
	DEC	72.5	61.8	−10.71	−14.76	22.46	−15.72	23.91	23.80

observations. In particular, the concentration peak that occurred on August 16th was well captured by the model. The model bias for NH_4^+, SO_4^{2-}, and NO_3^- were 0.11, 1.98, and −0.61 μg/m^3, respectively. The underestimation of NO_3^- was collaborated to the underestimation of NO_2 concentration. Overall, we have demonstrated the model's good ability in reproducing the concentrations of SO_2, NO_2, and the inorganic components of $PM_{2.5}$ in 2006.

The benefits of emission control policies on reducing SO_2 and SO_4^{2-} concentrations

In this sector, we investigated the change of SO_2 and SO_4^{2-} concentrations under the emission control policies adopted in the PS90 and P2010 scenarios. Figure 4 shows the annual average SO_2 concentration at the surface layer over the YRD region. Under the Base Case scenario (Fig. 4a), high SO_2 concentrations were found in northern Shanghai, where the main power plants and heavy industries were located. Another hot spot area was the city cluster formed by Suzhou, Wuxi, and Changzhou cities (S-W-C cluster) (Fig. 1b). Located in the southeast of Jiangsu province, this cluster is one of the fastest growing areas in China. In particular, the industrial gross output of Suzhou city has surpassed Shanghai and became number 1 in China in 2012. The SO_2 concentrations of these two areas were much higher than the other areas in the YRD region. This spatial distribution pattern agreed well with the previous study (Huang et al. 2014) that power plants and industries were the main contributors of SO_2 emissions in the YRD region.

Figure 4c and d show the change of SO_2 concentrations by implementing the idealized emission control policies described in the PS90 scenario. The amount of change in Fig. 4c was calculated as (Control Case − Base Case) and the percentage of change in Fig. 4d was calculated as ((Control Case − Base Case)/Base Case) × 100 %. Under the PS90 emission control scenario, the SO_2 concentration over the YRD region was reduced by an average of 8 μg/m^3 (51%), ranging spatially from 1 to 60 μg/m^3 (20–81%). The most pronounced benefits occurred in northern Shanghai,

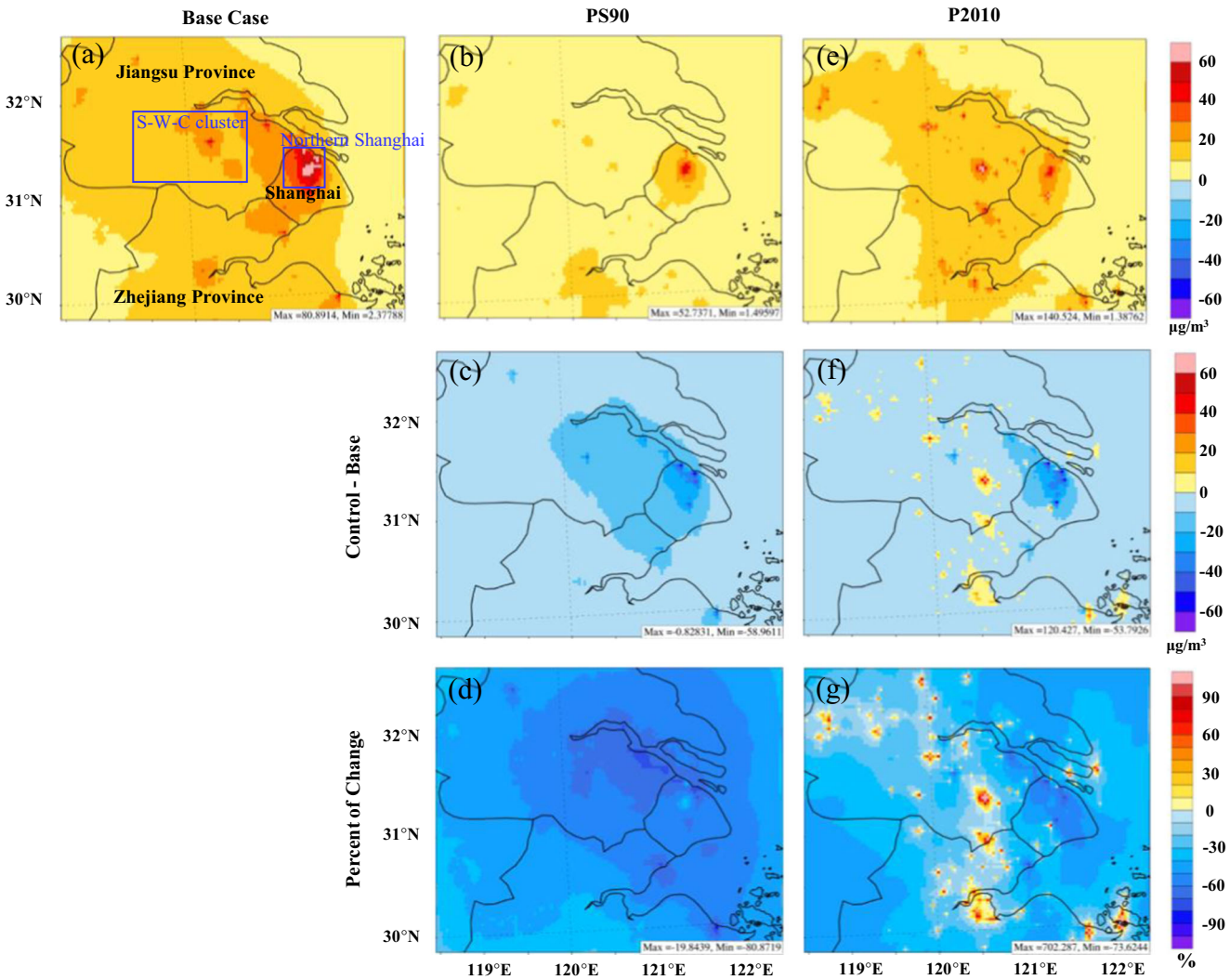

Fig. 4 SO_2 concentrations at ground level under **a** Base Case scenario, **b** PS90 control scenario, and **e** P2010 control scenario. Concentration changes between Base Case scenario and control scenario of **c** PS90 scenario and **f** P2010 scenario. Concentration changes in percentage between Base Case scenario and control scenario of **d** PS90 scenario and **g** P2010 scenario

where up to 60 μg/m^3 (78%) of SO_2 concentration was cut off. The impact on Jiangsu province was also significant, especially on the S-W-C cluster (~20 μg/m^3 and 60% reduction). However, the impact on Zhejiang province was lower than 10 μg/m^3 (40%).

Figure 4f and g show the amount of change and the percentage of change of SO_2 concentration under the P2010 scenario, which revealed the actual SO_2 reduction effects at the end of the 11th FYP. We found that the actual annual average reduction of SO_2 concentration was less than 5 μg/m^3 (30%) over the YRD region, with even increases at some areas. The reduction value ranges from 0 to 54 μg/m^3 (0–74%) spatially if not including the areas with increased SO_2 concentration. Figure S1 shows the spatial distribution of SO_2 emissions for Base Case (Fig. S1a) and P2010 (Fig. S1c). They used the emission from power plant in 2006 and 2010, but used the same emissions from other sectors. The difference between these two indicates the changes of emissions from power plants from 2006 to 2010 and the changes in the spatial pattern of power plants. Some grids located in Zhejiang and Jiangsu Province have higher SO_2 emissions in 2006 than 2010 due to that some power plants were newly built after 2006 or were not included in the 2006 emission inventory. The SO_2 concentration in these areas has increased from 2006 to 2010 (Fig. 4f).

The study of Wang et al. (2014) reported a reduction effectiveness of 37% for the 11th FYP control on SO_2 concentrations over the YRD region. However, Wang's study has included control measurements on industry boilers and residential sector besides the power plant sector. It is reasonable that the reduction effectiveness in this study is lower than Wang's. Comparing this scenario to the PS90 scenario, we found that the actual reduction of SO_2 concentrations were approximately 10 μg/m^3 (10–20%) lower than idealized value in most areas except northern Shanghai.

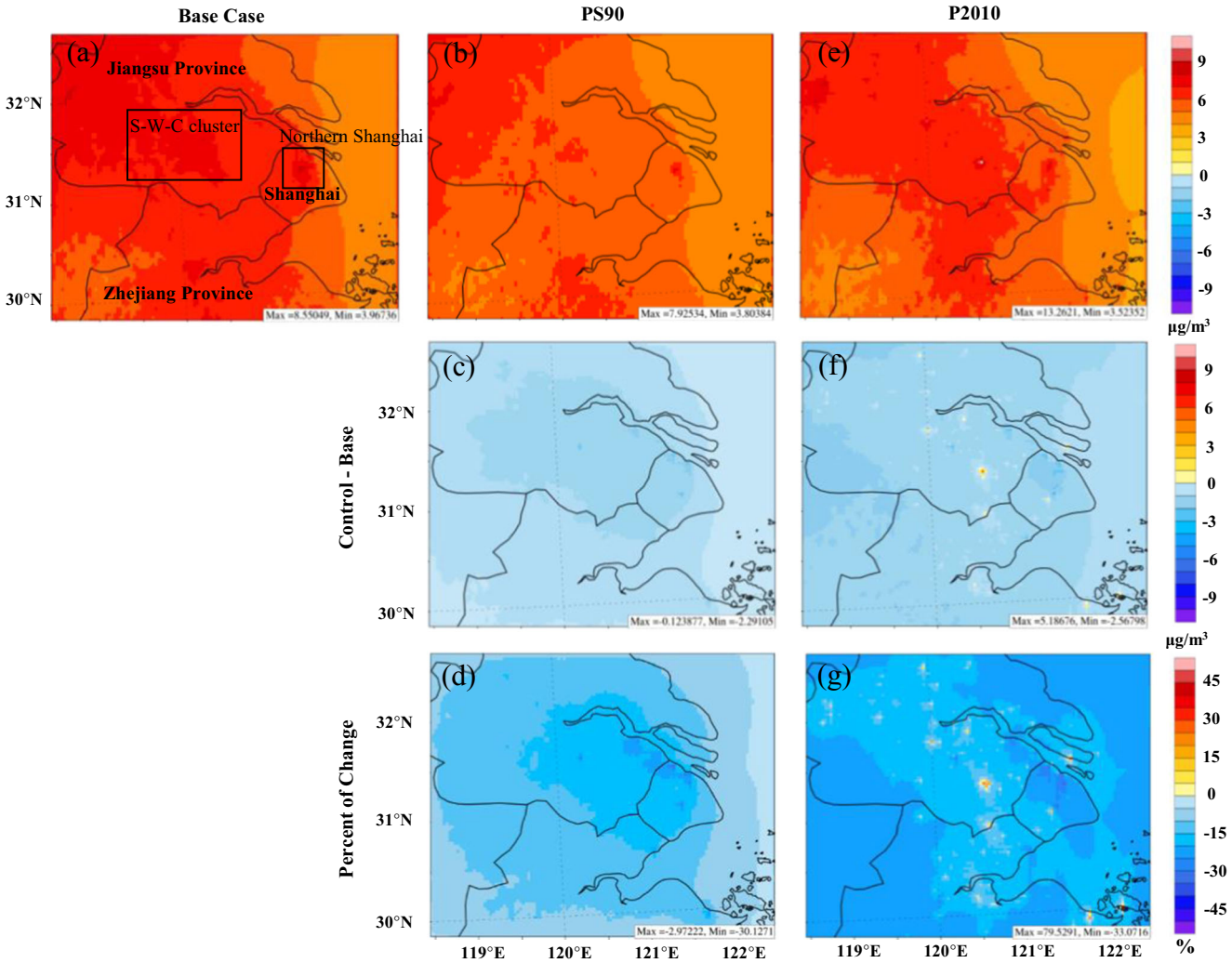

Fig. 5 SO_4^{2-} concentrations at ground level under **a** Base Case scenario, **b** PS90 control scenario, and **e** P2010 control scenario. Concentration changes between Base Case scenario and control scenario of **c** PS90 scenario and **f** P2010 scenario. Concentration changes in percentage between Base Case scenario and control scenario of **d** PS90 scenario and **g** P2010 scenario

Figure 5 illustrates the impact on SO_4^{2-} concentrations by control of SO_2 emission. Figure 5a shows the spatial distribution of SO_4^{2-} at the surface level. High concentrations were found in the northwest of Jiangsu province and northern Shanghai. The spatial distribution of SO_4^{2-} was somewhat different from SO_2. Meteorology condition is a possible reason since it is closely related to the dispersion of pollutants. Figure S3 shows the sulfur oxidation ratio (SOR), defined as $(SO_4^{2-}/(SO_4^{2-} + SO_2)) \times 100\%$, which could be regarded as a proxy of the oxidized extent of SO_2. The SOR was low (~10%) in the north of Shanghai, while it reached 40% in the northwest of Jiangsu province. In coastal cities like Shanghai, favorable meteorological conditions (such as sea breeze) facilitated the dispersion of air pollutants and reduced the sulfate oxidation reactions. As a consequence, higher SOR was found in the inland areas than the coastal areas. Another possible reason is the long-range transport from the west of the YRD region. We found high concentrations of SO_4^{2-} in the northwest of the YRD region and frequent transport of SO_4^{2-} in the air mass from that area (not shown in figure). These results agreed well with Zhang et al. (2015b) and Wang et al. (2006). The long-range transport is one of the main reasons of the high SO_4^{2-} concentration in the northwest of the YRD region.

Figure 5c and d show the reduction amount and reduction percentage of SO_4^{2-} concentrations under the PS90 scenarios. The effects of SO_2 emission control were less pronounced on SO_4^{2-} concentration than SO_2 concentration. The overall concentration of SO_4^{2-} was decreased by 0.9 μg/m^3 (0.1–2.2 μg/m^3) and 14% (3–30%) over the YRD region. The most pronounced changes occurred in northern Shanghai (30%) and the S-W-C cluster (24%). However, the SO_4^{2-} reduction in the northwest of Jiangsu province (5%) was below the average level despite the high SO_4^{2-} concentrations. Figure 5f and g

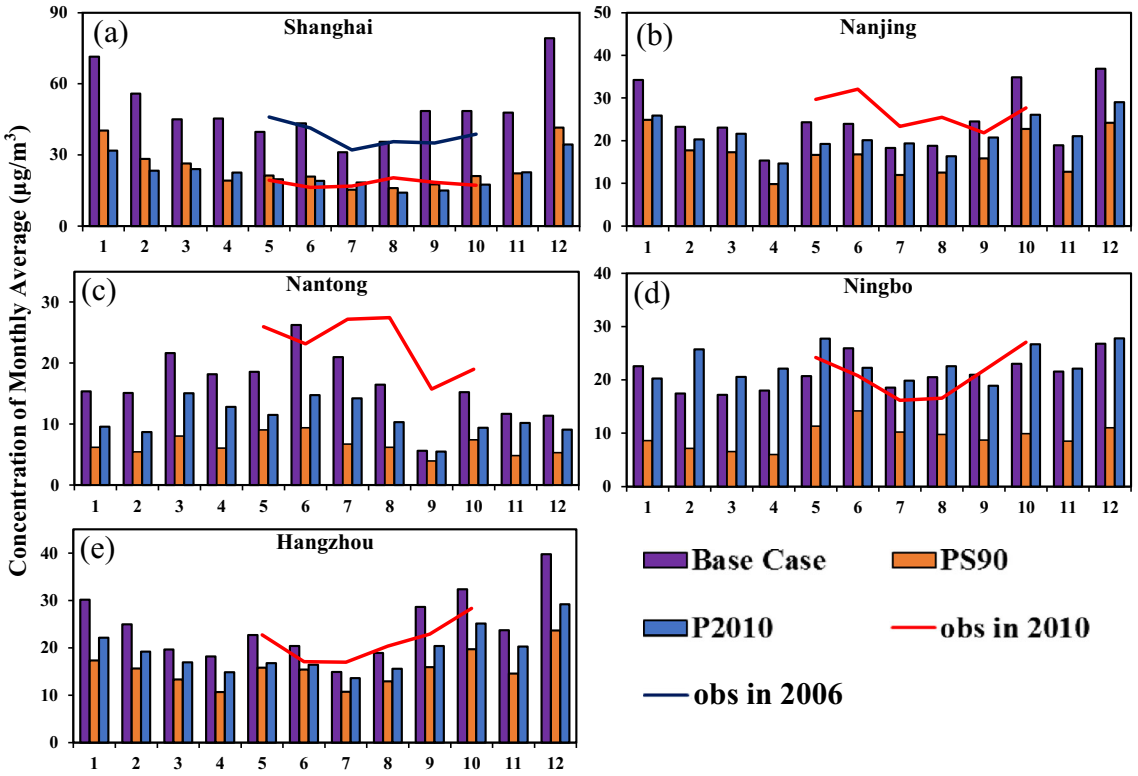

Fig. 6 Monthly average modeled SO_2 concentrations under Base Case, PS90, and P2010 emission control scenarios (*bars*) and observed SO_2 concentrations in 2006 and 2010 (*lines*) at **a** Shanghai, **b** Nanjing, **c** Nantong, **d** Ningbo, and **e** Hangzhou stations. Observed SO_2 concentrations in 2006 were only available at Shanghai station and observations in 2010 were available at all five stations

illustrate the results under the P2010 scenario. The actual reduction amount of SO_4^{2-} was approximately 0.6 μg/m^3 (9%) over the YRD region. The reduction value ranges spatially from 0 to 2.5 μg/m^3 (0–33%) if not including the areas with increased SO_4^{2-} concentration. Similar to SO_2, the real reduction effect under the P2010 scenario was generally 10% lower than the idealized value under the PS90 scenario.

This study did not include the impact of SO_2 emission control on NO_3^- and NH_4^+ concentrations. Although NO_3^- and SO_4^{2-} are competing species for NH_4^+, sufficient NH_3 emissions reduce the impact of SO_2 emission on the formation of NO_3^- for NH_3-rich regions, such as the YRD region (Dong et al. 2014; Wang et al. 2011).

The effectiveness of SO_2 emission control policies on power plants in major cities

In this section, we focused on five major cities in the YRD region, including Shanghai, Nanjing, Nantong, Ningbo, and Hangzhou. The measured SO_2 concentrations in Shanghai from May to October of 2006 were compared with those of 2010 in Fig. 6a. Other cities were not compared due to lack of

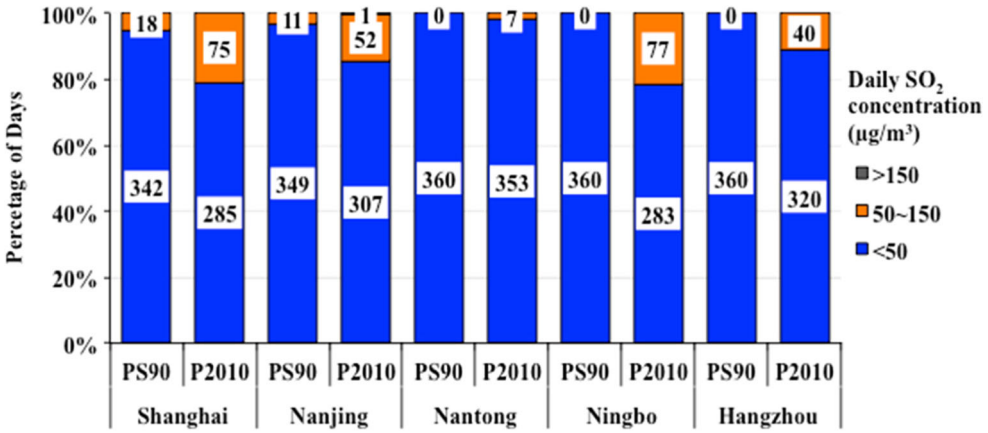

Fig. 7 Days at SO_2 concentration of <50, 50–150, and >150 μg/m^3 at Shanghai, Nanjing, Nantong, Ningbo, and Hangzhou stations under PS90 and P2010 scenarios. The label on the *bars* shows the number of days

2006 measurements. The observed SO_2 has decreased from 2006 to 2010 for all 6 months. However, this effect was partly contributed by the 11th FYP. Other control policies also have reduced the SO_2 emissions (e.g., the stringent emission control policies during the 2010 World Expo hosted by Shanghai; Huang et al. 2013).

To focus on the effects of the 11th FYP, we compared the model results under the Base Case and P2010 scenarios. Figure 6 shows the model results at Shanghai, Nanjing, Nantong, Ningbo, and Hangzhou stations. Differences between the two scenarios (calculated as ((P2010 − Base Case)/Base Case) × 100 %) indicated the effectiveness of the control policies implemented on power plants of the 11th FYP. Shanghai has the highest effectiveness of 55.1%, followed by Nantong (30.4%), Hangzhou (20.5%), and Nanjing (11.9%). However, a 10.7% increase of SO_2 concentration was found in Ningbo. This was due to increased SO_2 emissions from power plants in Ningbo after 2006, which was caused by expansion of old power plants in this city, such as Guodian Beilun Power Station, and newly built power plants, such as Huaneng Yuhuan Coal Power Plant (CARMA 2016). The observed SO_2 during May to October in 2010 was also presented in the figure for reference. For Shanghai, Ningbo, and Hangzhou, the modeled SO_2 concentrations under the P2010 scenario were close to the observation of 2010. However, for Nanjing and Nantong, the simulated SO_2 under the P2010 scenario were lower than the 2010 observation, probably because of the adverse meteorology condition or increased emissions from other sectors (e.g., industries) in these two cities.

The actual SO_2 reduction effectiveness (P2010) was generally lower than the optimal value (PS90) in most cities except Shanghai. The difference (calculated as (P2010 − PS90 scenario)) gave insight into the gap between the actual control effectiveness and the idealized value. For Shanghai, Nanjing, Nantong, Ningbo, and Hangzhou, the differences were −2.27 μg/m^3 (−9.4%), 4.27 μg/m^3 (25.2%), 4.37 μg/m^3 (66.8%), 13.71 μg/m^3 (146.9%), and 3.74 μg/m^3 (24.2%), respectively. The negative value for Shanghai presented good evidence on the proper implementation of the control policies in this city, while there were still large potentials for the other four cities to improve the working effectiveness of the control technologies. Working effectiveness of the control policies is influenced by several factors. First, the installation of FGD was a gradual process with spatial difference in the priority. The coverage of FGD technologies on power plants was 30% in 2006 and rose to 50% in 2007 (Zhang et al. 2015a) and the SO_2 removal rate increased from 25% in 2006 to 70% in 2010 (Yuan et al. 2013). As a consequence, areas that have early access to the control technologies have enjoyed more benefits than the others. Secondly, local reduction targets could also impact the reduction rates of emissions. According to the State Environmental Protection Administration (SEPA) of China, the total SO_2 emissions of 2005 were 513,000, 1373,000, and 860,000 t for Shanghai city, Jiangsu province, and Zhejiang province, while incomparably, the reduction targets were −26, −18, and −15% for the three cities/provinces, respectively (SEPA 2006). Another possible reason lies on how stringent the control policies were implemented. Big cities such as Shanghai might have higher control effectiveness. Shanghai seems to have reached the best control effect. However, whether this was realized by the control policies of the 11th FYP was questionable. During May 1st to October 31st in 2010, Shanghai hosted the 2010 Expo and extra stringent emission control policies have been implemented to keep the pollution level low. However, the air quality deteriorated sharply soon after the event (Hao et al. 2011; Huang et al. 2013). The short-term control policies have largely improved the air quality, but the effects have not stayed up long before the air pollution problem rebounded.

China's NAAQS is the ambient air quality standard released by the Ministry of Environmental Protection of China (MEP 2015). The NAAQS GB 3095-2012 is implemented with two classes of air quality standards. Class I is applied to special regions such as nature reserves and Class II is applied to the other areas including the residential, commercial, transportation, industrial, and rural areas. The annual limits of SO_2 concentrations for these two standards are 20 and 60 μg/m^3, respectively. Under the PS90 scenario (Fig. 4b), most of the YRD regions met the requirement of the Class II standard. While under the P2010 scenario (Fig. 4e), some industrial areas such as the S-W-C cluster and northern Shanghai exceeded Class II standard slightly. The daily limits of SO_2 concentrations for Class I and Class II are 50 and 150 μg/m^3, respectively. The numbers of days exceeding these two standards were calculated for Shanghai, Nanjing, Nantong, Ningbo, and Hangzhou under both PS90 and P2010 scenarios (Fig. 7). Under the PS90 scenario, the numbers of days exceeding Class I daily SO_2 standard was 18 (~5%), 11 (~3%), 0 (0%), 0 (0%), and 0 (0%) for Shanghai, Nanjing, Nantong, Ningbo, and Hangzhou, respectively. Under the P2010 scenario, the number of exceedance days increased to 75 (~21%), 52 (~14%), 7 (~2%), 77 (~21%), and 40 (~11%). In addition, Nanjing had 1 day that exceeded the Class II standard.

Conclusion

In this study, we conducted a post-assessment on the benefits and effectiveness of control policies of SO_2 emission on power plants during the 11th FYP (2006–

2010) over the YRD region. Evaluation of model performance showed the WRF and CMAQ model have well reproduced the meteorology field and air pollutants for 2006. SO_2 was generally well simulated with annual mean bias of −1.58 μg/m^3 (−23.30 to 13.89 μg/m^3) and RMSE of 30.80 μg/m^3 (14.75–32.09 μg/m^3). The model has captured most high concentration peaks. Three scenarios were designed according to the emission control policies implemented on power plants. Simulation results under the PS90 scenario, which assumed 90% SO_2 emission reduction from power plants, gave a prediction of 8 μg/m^3 (1–60 μg/m^3) and 51% (20–81%) reduction on SO_2 concentration and 0.9 μg/m^3 (0.1–2.2 μg/m^3) and 14% (3–30%) on SO_4^{2-} concentration over the YRD region from 2006 to 2010. However, the actual reduction of SO_2 concentration simulated under the P2010 scenario, which used the estimated SO_2 emissions from power plants in 2010, was around 5 μg/m^3 (0–54 μg/m^3) and 30% (0–74%) for SO_2 concentration and 0.6 μg/m^3 (0–2.5 μg/m^3) and 9% (0–33%) for SO_4^{2-} concentration. For most areas except Shanghai, the real SO_2 reduction effectiveness (P2010) was 10–20% lower than the idealized value (PS90).

For main cities in the YRD region, including Shanghai, Nanjing, Nantong, and Hangzhou, the actual effectiveness of SO_2 emission control policies on reducing SO_2 concentration were 55.1, 11.9, 30.4, and 20.5%, respectively. However, a 10.7% increase of SO_2 concentration was found in Ningbo due to expansion of old power plants and building of new power plants after 2006. The gaps between the actual control effectiveness and the optimal value (P2010 − PS90) were 25.2, 66.8, 146.9, and 24.2% in Nanjing, Nantong, Ningbo, and Hangzhou, respectively. There were large potentials for these four cities to improve the working effectiveness of emission control technologies. For Shanghai, the gap was −9.4%, which showed that Shanghai has reached the optimal emission control goal, but with the help of short-term control policies implemented during events like World Expo 2010. Appling the daily limits of SO_2 ambient concentration in China's NAAQS, we found that under the real SO_2 control condition (P2010), the exceeding day of Class I standard were 75 days (~21%), 52 days (~14%), 7 days (~2%), 77 days (~21%), and 40 days (~11%) for Shanghai, Nanjing, Nantong, Ningbo, and Hangzhou under P2010 scenario. The number could be decreased by 57 days (~16%), 41 days (~11%), 7 days (~2%), 77 days (~21%), and 40 days (~11%) if the control effectiveness is raised to the idealized level (PS90). This study investigated the working efficiencies of emission control policies at the end of the 11th FYP from a perspective of post-assessment. The results can serve as a scientific basis to assist the policy makers to improve air quality control strategies in the future.

Acknowledgements This work was partially supported by the National Science Foundation through TeraGrid resources provided by the National Institute for Computational Science (NICS) (TG-ATM110009 and UT-TENN0006). This work is supported by the National Natural Science Foundation of China (grant no. 41429501).

Compliance with ethical standards

Conflict of interest The authors declare that they have no competing interests.

Reference

Cao J, Garbaccio R, Ho MS (2009) China's 11th Five-Year Plan and the environment: reducing SO_2 emissions Rev Env Econ Policy 3:231–250 doi:10.1093/reep/rep006

CARMA (Carbon Monitoring for Action) (2016) Available from: http://carma.org/. Accessed 12 February 2016

Dong XY, Gao Y, Fu JS, Li J, Huang K, Zhuang GS, Zhou Y (2013) Probe into gaseous pollution and assessment of air quality benefit under sector dependent emission control strategies over megacities in Yangtze River Delta. China Atmospheric Environment 79:841–852. doi:10.1016/j.atmosenv.2013.07.041

Dong XY, Li J, Fu JS, Gao Y, Huang K, Zhuang GS (2014) Inorganic aerosols responses to emission changes in Yangtze River Delta, China. Science of the Total Environment 481:522–532. doi:10.1016/j.scitotenv.2014.02.076

Du Y (2008) New consolidation of emission and processing for air quality modeling assessment in Asia. M.S. thesis. University of Tennessee, Knoxville, TN

Fu X, Wang SX, Zhao B, Xing J, Cheng Z, Liu H, Hao JM (2013) Emission inventory of primary pollutants and chemical speciation in 2010 for the Yangtze River Delta region, China. Atmospheric Environment 70:39–50. doi:10.1016/j.atmosenv.2012.12.034

Han KM, Lee CK, Lee J, Kim J, Song CH (2011) A comparison study between model-predicted and OMI-retrieved tropospheric NO_2 columns over the Korean peninsula. Atmos Environ 45:2962–2971. doi:10.1016/j.atmosenv.2010.10.016

Han KM, Lee S, Chang LS, Song CH (2015) A comparison study between CMAQ-simulated and OMI-retrieved NO_2 columns over East Asia for evaluation of NOx emission fluxes of INTEX-B, CAPSS, and REAS inventories. Atmospheric Chemistry and Physics 15:1913–1938. doi:10.5194/acp-15-1913-2015

Hao N, Valks P, Loyola D, Cheng YF, Zimmer W (2011) Space-based measurements of air quality during the World Expo 2010 in Shanghai. Environ Res Lett 6. doi:10.1088/1748-9326/6/4/044004

Huang K, Fu JS, Gao Y, Dong XY, Zhuang GS, Lin YF (2014) Role of sectoral and multi-pollutant emission control strategies in improving atmospheric visibility in the Yangtze River Delta, China. Environ Pollut 184:426–434. doi:10.1016/j.envpol.2013.09.029

Huang K et al (2013) How to improve the air quality over megacities in China: pollution characterization and source analysis in Shanghai before, during, and after the 2010 World Expo. Atmos Chem Phys 13:5927–5942. doi:10.5194/acp-13-5927-2013

Lam YF, Fu JS (2009) A novel downscaling technique for the linkage of global and regional air quality modeling. Atmos Chem Phys 9:9169–9185

Lin YF, Huang K, Zhuang GS, Fu JS, Xu C, Shen JD, Chen SY (2013) Air quality over the Yangtze River Delta during the 2010 Shanghai Expo. Aerosol Air Qual Res 13:1655-+. doi:10.4209/aaqr.2012.11.0312

MEP (Ministry of Environmental Protection of the People's Republic of China) (2015) Available from: http://www.mep.gov.cn/image20010518/5298.pdf. Accessed 12 February 2016

Schreifels JJ, Fu YL, Wilson EJ (2012) Sulfur dioxide control in China: policy evolution during the 10th and 11th Five-Year Plans and lessons for the future. Energy Policy 48:779–789. doi:10.1016/j.enpol.2012.06.015

SCPRC (State Council of People's Republic of China) (2006) National 11th Five Year Plan on Environmental Protection. Available from: http://www.gov.cn/ztzl/2006-03/16/content_228841_7.htm. Accessed 12 February 2016

SEMC (Shanghai Environmental Monitoring Center) (2015). Available from: http://www.envir.gov.cn/airnews/index.asp. Accessed 12 February 2016

SEPA (State Environmental Protection Administration) (2006) 2006 Report on the State of the Environment in China. Available from: http://english.mep.gov.cn/down_load/Documents/200710/P020071023479580153243.pdf?COLLCC=4155369982&

Srivastava RK, Jozewicz W (2001) Flue gas desulfurization: the state of the art. Journal of the Air & Waste Management Association 51:1676–1688

Srivastava RK, Jozewicz W, Singer C (2001) SO_2 scrubbing technologies: a review. Environ Prog 20:219–227. doi:10.1002/Ep.670200410

Streets DG, Waldhoff ST (2000) Present and future emissions of air pollutants in China: SO_2, NO_x, and CO. Atmos Environ 34:363–374. doi:10.1016/S1352-2310(99)00167-3

Wang LT et al (2010a) Assessment of air quality benefits from national air pollution control policies in China. Part I: background, emission scenarios and evaluation of meteorological predictions. Atmos Environ 44:3442–3448. doi:10.1016/j.atmosenv.2010.05.051

Wang LT et al (2010b) Assessment of air quality benefits from national air pollution control policies in China. Part II: evaluation of air quality predictions and air quality benefits assessment. Atmos Environ 44:3449–3457. doi:10.1016/j.atmosenv.2010.05.058

Wang LT et al (2013a) Assessment of urban air quality in China using air pollution indices (APIs). J Air Waste Manage Assoc 63:170–178. doi:10.1080/10962247.2012.739583

Wang S, Xing J, Jang C, Zhu Y, Fu JS, Hao J (2011) Impact assessment of ammonia emissions on inorganic aerosols in East China using response surface modeling technique. Environmental science & technology 45:9293–9300. doi:10.1021/es2022347

Wang SX, Hao JM (2012) Air quality management in China: issues, challenges, and options. J Environ Sci-China 24:2–13

Wang SX, Xing J, Zhao B, Jang C, Hao JM (2014) Effectiveness of national air pollution control policies on the air quality in metropolitan areas of China. J Environ Sci-China 26:13–22

Wang SX et al (2010c) Quantifying the air pollutants emission reduction during the 2008 Olympic Games in Beijing. Environmental science & technology 44:2490–2496

Wang Y, Hao J, McElroy MB, Munger JW, Ma H, Chen D, Nielsen CP (2009) Ozone air quality during the 2008 Beijing Olympics: effectiveness of emission restrictions. Atmos Chem Phys 9:5237–5251

Wang Y, Zhang QQ, He K, Zhang Q, Chai L (2013b) Sulfate-nitrate-ammonium aerosols over China: response to 2000–2015 emission changes of sulfur dioxide, nitrogen oxides, and ammonia. Atmos Chem Phys 13:2635–2652

Wang Y et al (2006) The ion chemistry, seasonal cycle, and sources of PM2.5 and TSP aerosol in Shanghai. Atmos Environ 40:2935–2952. doi:10.1016/j.atmosenv.2005.12.051

Xing J et al (2011a) Projections of air pollutant emissions and its impacts on regional air quality in China in 2020. Atmos Chem Phys 11:3119–3136

Xing J et al (2011b) Modeling study on the air quality impacts from emission reductions and atypical meteorological conditions during the 2008 Beijing Olympics. Atmos Environ 45:1786–1798

Xu YA (2011) Improvements in the operation of SO_2 scrubbers in China's coal power plants. Environmental science & technology 45:380–385

Xue WB et al (2013) Assessment of air quality improvement effect under the National Total Emission Control Program during the Twelfth National Five-Year Plan in China. Atmos Environ 68:74–81

Yuan XL, Mi M, Mu RM, Zuo J (2013) Strategic route map of sulphur dioxide reduction in China. Energ Policy 60:844–851

Zhang Q et al (2009) Asian emissions in 2006 for the NASA INTEX-B mission. Atmos Chem Phys 9:5131–5153

Zhang QQ, Wang Y, Ma Q, Yao Y, Xie Y, He K (2015a) Regional differences in Chinese SO_2 emission control efficiency and policy implications. Atmos Chem Phys 15:6521–6533

Zhang XY, Wang JZ, Wang YQ, Liu HL, Sun JY, Zhang YM (2015b) Changes in chemical components of aerosol particles in different haze regions in China from 2006 to 2013 and contribution of meteorological factors. Atmos Chem Phys 15:12935–12952. doi:10.5194/acp-15-12935-2015

Zhao Y, Wang SX, Duan L, Lei Y, Cao PF, Hao JM (2008) Primary air pollutant emissions of coal-fired power plants in China: current status and future prediction. Atmos Environ 42:8442–8452